

Hydrolysis of Ferric Ion in Water and Conformational Equilibrium

Richard L. Martin, P. Jeffrey Hay, and Lawrence R. Pratt

Theoretical Division, Los Alamos National Laboratory, Los Alamos, New Mexico 87545 USA

LA-UR-97-3489

(March 24, 2018)

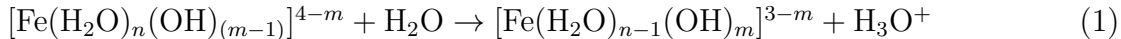
Abstract

Reported here are results of theoretical calculations on $\text{Fe}(\text{H}_2\text{O})_6^{3+}$, $\text{Fe}(\text{H}_2\text{O})_5(\text{OH})^{2+}$, three isomers of $\text{Fe}(\text{H}_2\text{O})_4(\text{OH})_2^+$, and $\text{Fe}(\text{H}_2\text{O})_3(\text{OH})_2^+$ to investigate the molecular mechanisms of hydrolysis of ferric ion in water. The combination of density functional electronic structure techniques and a dielectric continuum model for electrostatic solvation applied to the $\text{Fe}(\text{H}_2\text{O})_6^{3+}$ complex yields an estimate of -1020 kcal/mol (experimental values -1037 kcal/mol to -1019 kcal/mol) for the absolute free energy of the aqueous ferric ion. The free energy change for the first hydrolysis reaction is predicted reasonably (2 kcal/mol predicted compared to 3 kcal/mol experimental). For the second hydrolysis reaction, we found an unexpected low energy isomer of $\text{Fe}(\text{H}_2\text{O})_4(\text{OH})_2^+$ with five ligands in the inner sphere and one water outside. The hexa-coordinate *cis* and *trans* isomers are, respectively, slightly lower and higher in energy. Calculations on the penta-coordinate species $\text{Fe}(\text{H}_2\text{O})_3(\text{OH})_2^+$ suggest that extrusion of the outer sphere water is nearly thermoneutral. The reaction free energy for the second hydrolysis is predicted in the range 16-18 kcal/mol, higher than the experimental value of

5 kcal/mol. In view of the facts that the theoretical predictions are higher than experimental values, and that novel structures were encountered among products of the second hydrolysis, we argue that conformational entropy is an important omission in this theoretical treatment of net reaction free energies. A fuller cataloging of low energy hydrolysis products and direct calculations of partition functions of the isolated complexes should help in modeling equilibrium speciation in groundwaters.

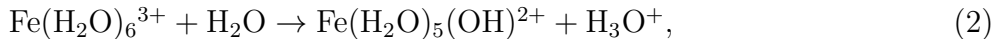
1. Introduction

A molecular theoretical account of the free energetics of the reactions



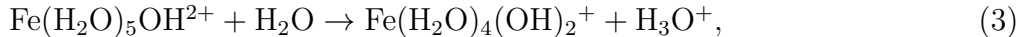
in water can benefit from discrimination of the conformers that are present under common conditions. Entropic contributions to the solution thermodynamics may reflect multiple configurations that occur. Thus information on the conformers present should assist in accurately describing temperature variations of solvation properties. In addition, theoretical study of the molecular structure of the species participating these reactions should teach us about the molecular mechanisms involved and provide a benchmark of current theoretical tools for modeling speciation of metal ions in groundwaters [1,2,3].

The condition of ferrous and ferric ions in solution has long been of specific interest to explanations of electron exchange processes [4,5,6,7]. The hydrolysis product $\text{Fe}(\text{H}_2\text{O})_5\text{OH}^{2+}$ often contributes significantly to the rate of ferric ion reduction in water because the specific rate constant for ferric-ferrous electron exchange is about a thousand times larger for the hydrolyzed compared to unhydrolyzed hexaaquoferrous ion [8]. The net standard free energy change (about 3 kcal/mol [9]) for the first hydrolysis reaction,



is small compared to the size of the various contributions that must be considered in theoretical modeling of these solution species.

In contrast to the great volume of work on electron transfer involving such species, reactions of particular interest here transfer a proton from a water ligated to a Fe^{3+} ion to a free water molecule. The second hydrolysis,



raises more seriously the possibility of participation by several isomers in the mechanism and thermodynamics of these reactions.

This work takes ferric ion hydrolysis as a demonstration system for determination of the utility of current theoretical tools for modeling of speciation of metal ions in aqueous solution. At this stage we have not considered multiple metal center aggregates. We report below encouraging agreement with experimental thermochemistries but with unexpected results that must be addressed for further progress in describing these chemical systems in molecular terms.

2. Approach

The physical idea of treating an inner solvation shell on a different footing from the rest of the solvent has considerable precedent [10]. Friedman and Krishnan referred to these approaches as *hybrid models* and criticized them on the grounds that individual contributions to the thermodynamic properties of final interest could not be determined with sufficient accuracy to draw new conclusions from the final results. However, particularly for highly charged and chemically complex ions, the hybrid approaches seem indispensable [11]. Computational and conceptual progress in the 25 years since that Friedman-Krishnan review has made these approaches interesting once again. In what follows, we first elaborate on the calculational techniques used. An appendix discusses some of the statistical thermodynamic issues underlying these hybrid models.

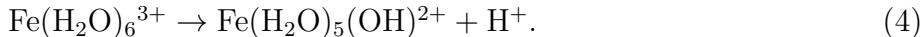
2.1. Electronic Structure Calculations

Reliable estimation of free energies of dissociation in aqueous media requires a similarly reliable determination of the process in the gas phase. Given the well known difficulties associated with electron correlation in transition metal complexes, and our intent to extend this work to larger and more complex systems, we chose to explore this problem with the B3LYP hybrid density functional theory (DFT) [12,13]. This approximation is an effective compromise between accuracy and computational expense, and has been shown to give usefully accurate predictions of metal-ligand bond energies in a number of molecules [14,15]. In the present application however, we were less interested in the metal-ligand bond energy

than in the energies for successive elimination of protons from the H₂O ligands bound to Fe³⁺. This may be a somewhat less severe test of the functional. The details of our approach and estimates of the errors follow.

The geometry and vibrational frequencies of the metal complex were determined using the 6-311+G basis set for the metal ion and the 6-31G* basis set for the ligands [13]. The former is contracted from Wachters' [16] primitive Gaussian basis (including the functions describing the 4s and 4p atomic orbitals) and augmented with the diffuse d-function of Hay [17]. The ligand basis set contains a polarization function of d-character on the oxygen. At the optimum geometry, a single calculation was done to determine the energy in a more extended basis (6-31++G**) that includes polarization and diffuse functions on both the oxygen and hydrogen centers. Atomic charges were determined in this extended basis as well using the ChelpG [18] capability ($R_{Fe}=2.02 \text{ \AA}$) in the Gaussian94 package [13]. All Fe species are high-spin (d⁵) treated in the spin-unrestricted formalism.

One might argue, on the basis of the OH⁻ character expected in the product complexes, that the geometry optimization should also be done with a diffuse basis set for the ligands. This was found unnecessary by explicit calculations on the partial reaction



The endothermicity of this reaction computed from a single point calculation with the 6-31+G* basis at its optimum geometry differs by only 0.2 kcal/mole from the result obtained with the smaller basis. More important are additional polarization and diffuse functions on the hydrogens; for example, neglecting zero-point corrections, the B3LYP endothermicities are 29.2 kcal/mole(6-31G*), 25.4 kcal/mole(6-31+G*), and 28.1 kcal/mole(6-31++G**).

A final consideration regarding basis set convergence is the importance of polarization (f-functions) on the metal center. This was examined by augmenting the 6-311+G Fe basis with two f-functions ($\alpha = 0.25, 0.75$) split about a value ($\alpha = 0.4$) optimized for Fe(H₂O)₆³⁺. In this larger basis an endothermicity of 27.9 kcal/mole results compared to the value 28.1 kcal/mole obtained without the f-functions. The correction to the second

hydrolysis is only slightly larger, ~ 0.5 kcal/mole. We thus conclude that the B3LYP deprotonation energies are nearly converged with respect to further improvements in the basis set. A conservative estimate might be associated with the change observed between the 6-311+G/6-31+G* results and the 6-311+G(2f)/6-31++G** results, or about 2-3 kcal/mole.

Convergence of the results with respect to basis set does not address the accuracy expected with the B3LYP method. In so far as the water molecules retain their identity when bound to the metal ion, we expect the error in the hydrolysis reaction to be approximated by the error observed for the analogous reaction for a single H₂O molecule. The procedure outlined above was therefore used to determine the energies and zero-point energies (ZPE) for a number of species associated with the neutral and ionic dissociation channels of H₂O. They are reported in Table I, and can be used to determine the properties and reaction energies reported in Table II. The H₂O thermochemistries shown there are in excellent agreement with experiment. For example, the error associated with the reaction



is underestimated by less than 2 kcal/mole. The errors in the other dissociation channels are similar.

2.2. Electrostatic Solvation Calculations

Electrostatic interactions of hydrated ferric ions with the aqueous environment are expected to be of first importance in this solution chemistry. These hydrolysis reactions are written so that other contributions to the net free energy, *e.g.* packing, might balance reasonably. Thus, continuum dielectric solvation modeling is a reasonable approach to studying these solution processes; it is physical, computationally feasible, and can provide a basis for more molecular theory [19,20,21,22,23,24,25,26,27,28,29]. The dielectric model produces an approximation to the interaction part of the chemical potential, μ^* of the solute; in notation used below $\mu^* = -RT \ln \langle \exp(-\Delta U) \rangle_0$ where for this case ΔU is the solute-solvent electrostatic interaction potential energy and the brackets indicate the

average over the thermal motion of the solvent uninfluenced by the charge distribution of the solute [19,20,21,22,23,24,27,29]. Free energy contributions due to non-electrostatic interactions are neglected. We address free energy changes due to atomic motions internal to the complexes on the basis of gas phase determinations of the vibrational frequencies and partition functions. The solvation calculation treats all species as rigid; we comment later on the consequences of this approximation and on the possibilities for relaxing it . The solute molecular surface was the boundary between volume enclosed by spheres centered on all atoms and the exterior. The sphere radii were those determined empirically by Stefanovich [30], except $R_{Fe}=2.08 \text{ \AA}$ for the ferric ion. The ferric ion is well buried by the ligands of these complexes and slight variations of this latter value were found to be unimportant. The numerical solutions of the Poisson equation were produced with a boundary integral procedure as sketched in references [23,27] typically employing approximately 16K boundary elements. The accuracy of the numerical solution of the dielectric model is expected to be better than a kcal/mol for the electrostatic solvation free energy.

3. Results and Discussion

The pertinent energies for $\text{Fe}(\text{H}_2\text{O})_6^{3+}$ and other species involved in hydrolysis processes are compiled in Tables I and II. The magnitudes of the various components entering into the gas phase hydrolysis free energy are reported in Table III, while Table IV adds the solvation contributions to the free energy and compares the total with experiment. Table V summarizes geometrical information and partial atomic charges computed from the electrostatic potential fit are presented in Table VI.

3.1. $\text{Fe}(\text{H}_2\text{O})_6^{3+}$

The structure of the $\text{Fe}(\text{H}_2\text{O})_6^{3+}$ complex, T_h symmetry, is shown in Figure 1. The B3LYP approximation gives an Fe-O distance of 2.061 \AA . By way of comparison, with the identical basis set the Hartree-Fock approximation yields 2.066 \AA . These distances are similar to the recent Hartree-Fock results of Åkesson, *et al.* [31], $R_{FeO} = 2.062 \text{ \AA}$,

and the gradient-corrected DFT(BPW86) calculations of Li, *et al.* [32], $R_{FeO} = 2.067 \text{ \AA}$. These theory values cluster in the upper end of the range of distances ($1.97 \text{ \AA} - 2.05 \text{ \AA}$) determined experimentally [33,34,35]. Neutron scattering measurements report 2.01 \AA in concentrated electrolyte solutions [33]. The solution EXAFS result (1.98 \AA) is close to the crystallographic determinations, $1.97 \text{ \AA} - 2.00 \text{ \AA}$ [34]. In their recent review, Ohtaki and Radnai discuss a number of other experiments and conclude the distance lies in the range of $2.01 - 2.05 \text{ \AA}$ [35].

Though these theory values are compatible with the upper end of this range, they are far from the EXAFS result (1.98 \AA) that might be the most reliable experimental determination. While investigating this question, we found that the B3LYP value is stable with respect to further improvements in the basis; if the basis is augmented with an f-function on the metal and diffuse functions on the oxygens, the equilibrium distance decreases only slightly ($R_{Fe-O} = 2.053 \text{ \AA}$). As noted above, the B3LYP result is in close agreement with that from the Hartree-Fock approximation. It would not be surprising, however, if the HF approximation overestimated the bond length. Akesson, *et al.* [36,37] have previously observed that the HF bond lengths for a series of first row transition metal hydrates are systematically too long. They find that correlation effects and the influence of the second hydration shell each act to reduce the bond length by about 0.01 \AA . Even with these corrections the theoretical bond length is still much larger than 1.98 \AA . As an additional data point, the local-density-approximation with the present basis yields $R_{Fe-O} = 2.013 \text{ \AA}$, in better agreement with the EXAFS and crystallographic determinations. However, while the LDA generally gives reasonable geometries for transition metal complexes [38,39], Sosa, *et al.* [39] find that it tends to underestimate the lengths of dative bonds, such as the one discussed here, and this might further support a bond length toward the upper end of the range.

The atomic partial charges computed here for the hexaaquoferric ion are given in Table VI. Note that the charge assigned to the ferric ion is substantially less than $3e$, and that the magnitudes of the charges on the oxygen and hydrogen atoms are substantially greater

than is common with effective force fields used for simulation of liquid water.

As discussed in the appendix, a value for the absolute free energy of the ferric ion can be obtained from a free energy of formation of the $\text{Fe}(\text{H}_2\text{O})_6^{3+}$ complex from an isolated Fe^{3+} (6S) ion and six water molecules (Table III), provided that no solvation contribution is included for the atomic ion and that the actual, not standard state, species concentrations are used. That absolute free energy in aqueous solution is -1020 kcal/mol. Experimental values range from -1037 kcal/mol to -1019 kcal/mol [40,41,10,42]. We note that this theoretical value takes no account of solvation effects due to non-electrostatic interactions.

This agreement with experiment is encouraging. In computing the absolute free energy there are a number of large contributions to the final result. This contrasts to the hydrolysis reactions where we have arranged things to encourage cancellation of errors. It is interesting to examine the components contributing to the free energy in the gas phase (Table III). Not surprisingly, the zero-point correction, +15 kcal/mole, is significant. Under the standard conditions, hypothetical $p=1$ atm ideal gas with $T=298.15$ K, there is the large, unfavorable differential entropy contribution, +47 kcal/mole. This arises from the necessity of sequestering six water molecules in a dilute gas. The net free energy found for the gas phase reaction is -602 kcal/mole. Table IV addresses the solution phase aspects of this thermochemistry. (See the Appendix also.) About half of the ideal entropy penalty mentioned is regained in the liquid because of the higher concentration of water molecules. The differential solvation free energy adds another -391 kcal/mole of (favorable) free energy for a net absolute free energy of hydration of -1020 kcal/mole.

This estimate of the absolute free energy of the ferric ion is close to the value -1037 kcal/mole reported by Li, *et al.* [32] as a hydration *enthalpy*. The Li, *et al.*, value contains some terms that would be appropriate if the hydration enthalpy were sought and some terms that would contribute to the hydration free energy; thus comparison of that previous value with the present result is not straightforward. In fact, the most pragmatic calculation of the hydration enthalpy within the dielectric continuum model is nontrivial. The enthalpy would be then obtained by determining a temperature derivative of the chemical potential.

The appropriate temperature derivative determines the enthalpy directly or, alternatively, the solvation entropy so that the desired enthalpy might be determined by differencing with the already known chemical potential. That temperature derivative would generally involve also the temperature variation of the radii-parameters [19,20,21,27,29]. The variations with thermodynamic state of the radii-parameters have not been well studied [21]. There is good agreement, however, in many of the components contributing to this hydration enthalpy. Li, *et al.*, report a gas phase energy of formation of -652.2 kcal/mole with the BPW86 gradient-corrected functional compared to the present B3LYP result of -655.2 kcal/mole, and their solvation free energy is -444 kcal/mole *vs.* the -441 kcal/mole found here. Such close agreement is encouraging, although somewhat fortuitous. Our gas phase energy of formation includes a correction, not considered by Li, *et al.*, of some 15 kcal/mole for the zero-point energies. It is encouraging, however, that the estimates disagree by only about 15 kcal/mole, or some 1.5%. Additionally, the definition of the molecular surface adopted by Li, *et al.*, for the solvation calculation was substantially different from that used here, as were the radii-parameters used.

3.2. First and second hydrolysis reactions

We turn now to the first deprotonation reaction Eq. 2. The structure found for $\text{Fe}(\text{H}_2\text{O})_5\text{OH}^{2+}$ is displayed in Figure 2. The Fe-O (hydroxide) distance is 1.76 Å and the Fe-O (water) distances lengthen to 2.10 Å – 2.15 Å. Assembling the results for the standard free energy of this reaction we find 2 kcal/mol, in surprisingly good agreement with the experimental value of 3 kcal/mol [9]. This computed net free energy change is composed of approximately -148 kcal/mol exothermic (favorable) change in isolated molecule free energy and +150 kcal/mol (unfavorable) net increase in solvation free energy. The solvation contribution favors the reactant side here because it presents the most highly charged ion. Changes in the radius assigned to the iron atom in the range $2.06 \text{ \AA} \leq R_{\text{Fe}} \leq 2.10 \text{ \AA}$ lead to changes of ± 1 kcal/mol in the predicted reaction free energy. This reaction was also considered by Li, *et al.*, [32] who find it to be exothermic by 14 kcal/mole.

To treat the next hydrolysis Eq. 3 we must consider $\text{Fe}(\text{H}_2\text{O})_4(\text{OH})_2^+$ species. Figure 3 shows the stable structures found. Further lengthening of both the Fe-O(water) and Fe-O(hydroxide) distances is noted (Table V) in the *cis* and *trans* six-coordinate species by 0.07-0.14 Å compared to the $\text{Fe}(\text{H}_2\text{O})_5\text{OH}^{2+}$. In the gas phase, the *cis* structure is predicted to be the lowest energy conformer, slightly (1 kcal/mole) below the *trans* isomer. This preference is reversed in solution, where the *trans* isomer is predicted to be slightly more stable. We note that the most current force fields applied to simulation of ferric ions in solution place the *cis* structure significantly higher in energy than the *trans* [3].

We were surprised to discover a stable *outer* sphere complex during our search for the stable *trans* structure. The structure is given in Figure 3. The distances between the hydroxyl oxygens and the outer sphere water are typical of hydrogen bonds. Explicit calculation of the vibrational frequencies show it to be a true local minimum, lying less than a kcal/mol higher in energy than the *cis* conformer.

The interaction of the outer sphere water with the remainder of the ferric hydrate complex can be partially characterized by finding the energy of that complex without the outer sphere partner. The structure obtained for that penta-coordinate ferric ion is shown in Figure 4. The penta-coordinate complex can stably adopt a conformation similar to that of Figure 3 also in the absence of the outer sphere water. In terms of the zero-point corrected electronic energy, this *outer* sphere complex is stable with respect to loss of the H_2O by about 7 kcal/mole. Consideration of the entropic contributions to the free energy find the complex still stable with respect to loss of H_2O , but the differential solvation contributions reverse this conclusion. Thus, the dissociation of the outer sphere complex is an essentially thermoneutral process. We suspect such intermediates play an important role in the mechanism of the ligand exchange with the solvent.

These three conformers lead to estimates of 16 kcal/mol, 16 kcal/mol, and 18 kcal/mol for the reaction free energy of the second hydrolysis for *trans*, *outer*, and *cis sphere* products, respectively; the experimental value is approximately 5 kcal/mol [9,43]. We note that as in the case of the first hydrolysis, the gas phase predictions lead to an exothermic reaction; it

is the differential solvation free energy that tips the scales in favor of endothermicity.

3.3. Role of conformational entropy

The issue of the internal motions of the complexes, and the near degeneracy of several conformers, raises also the issue of conformational entropy of these species. For example, in the second hydrolysis reaction, factors such as $-RT\ln 3$ arise if the three isomers discussed here are considered isoenergetic. [However, the multiplicity of isoenergetic states will surely not be just 3 and, furthermore, entropy *differences* are required here.] As another example, the T_h hexaaquo complex surely has a number of low-lying structures involving the rotation of the plane of an individual H_2O . More generally, this conformational entropy would be appropriately included by computing the solvation contribution to the chemical potential, μ^* , of the complex according to

$$\mu^* = -RT \ln \sum_c x_c^{(0)} e^{-\mu^*(c)/RT} \quad (6)$$

where the sum indicated is over conformations c weighted by the normalized population, the mole fractions $x_c^{(0)}$ of conformers when there is no interaction between solute and solvent, and further the summand is the Boltzmann factor of the solvation free energies, perhaps from a physical model such as the dielectric model used here, for each conformation. [The treatment of the thermodynamics of flexible complexes in solution is also discussed further in the appendix and in Reference [44].] The solvation contribution to the chemical potential Eq. 6 would then be combined with the isolated cluster partition function to obtain the free energies of the species involved and free energy changes for the reactions [44]. Finally, an entropic contribution, including any conformational entropy, would be obtained by temperature differentiation of the full chemical potential. The isolated cluster partition functions would properly include an entropy associated with the multiplicity of isoenergetic conformational states. It is reasonable to expect that this conformational entropy increases progressively with hydrolysis, *i.e.* the products here are “less ordered,” and have higher conformational entropy than their reactants. It is thus significant that the predicted reaction

free energies are higher than the experiment; inclusion of conformational entropy should lower these reaction free energies.

We note that Li, *et al.* [32] argue that inclusion of a second solvation shell substantially improves the accuracy of the thermochemical predictions. The present results do not seem to force us to larger clusters. Although it is true that proper inclusion of more water molecules should permit a more convincing treatment, inclusion of more distant water molecules makes the neglect of conformational entropy less tenable. In any case, comparison of dielectric model treatments with thermochemical results only permits limited conclusions because of the empirical adjustability of radii-parameters.

4. Conclusions

Given the balance of the large contributions that must be considered, the observed accuracy of the computed hydrolysis reaction free energies reactions is encouraging. Evidently many structural possibilities will have to be treated for a full description of ferric ion speciation in water, eventually considering higher aggregates and anharmonic vibrational motions of the strongly interacting water molecules and other ligands. These issues are probably best pursued through development of a molecular mechanics force field to screen structures rapidly, reserving electronic structure calculations for verification of the important structures found and refinement of the force field. The energetic ordering found here for isomers of $\text{Fe}(\text{H}_2\text{O})_4(\text{OH})_2^+$ is *cis* (lowest), *outer sphere*, and *trans* (highest), but all these energies are within about 2 kcal/mol. Molecular mechanics force fields might be reparameterized to account for these results [1,2,3]. Identification of prominent isomers should simplify and improve the modeling of the temperature variations of thermodynamic properties. It deserves emphasis also that substantial contributions to these reaction free energies, and to the accumulated uncertainties, are associated with the water partners in these reactions, *i.e.* the free energies associated with solvation of H_2O and H_3O^+ . A similar comment would apply for other common oxy-acids and ligands in water, *e.g.* carbonate, nitrate, sulfate, and phosphate. Molecular descriptions of metal ion speciation will be incomplete without

accurate molecular characterizations of these species in aqueous solution.

Acknowledgement

This work was supported by the LDRD program at Los Alamos. LRP thanks Marshall Newton for helpful discussions on these topics.

APPENDIX

Here we specify with greater care some of the statistical thermodynamic considerations relevant to solvation free energies obtained from cluster calculations of the present variety [13]. We note that these issues are of minor importance for the hydrolysis reactions that are the focus of this paper. However, these considerations become more important for the absolute free energy reported for the aqueous ferric ion and for the free energy of dissociation of the outer sphere complex.

Utilizing calculations on clusters

We first specify more fully and explain the procedure from computing the absolute free energy of the ferric ion given in Table IV on the basis of cluster results obtained from density functional theory and the dielectric continuum estimate of solvation contributions. The result of the development here is a formula for the chemical potential of the ferric ion:

$$\mu_{Fe^{3+}} = RT \ln \left[\frac{\rho_{Fe^{3+}} V}{q_M \langle \langle e^{-\Delta U/RT} \rangle \rangle_{0,M}} \right] - 6\mu_W, \quad (7)$$

Here $\rho_{Fe^{3+}}$ the number density of ferric ions in the solution, V is the volume of the system, q_M is the partition function of the isolated hexaaquoferric complex ($M=Fe(H_2O)_6^{3+}$), $-RT \ln \langle \langle e^{-\Delta U/RT} \rangle \rangle_{0,M}$ is the solvation free energy of the complex, and μ_W is the chemical potential of the water. The conclusion drawn from this formula is that the desired absolute free energy of the hydrated ferric ion is obtained from the chemical potential change of the reaction $Fe^{3+} + 6H_2O \rightarrow Fe(H_2O)_6^{3+}$ except with the additional provisions that the chemical

potentials should be evaluated on a fully molecular basis at the water concentration of interest and no solvation contribution should be included for the atomic ion. The subsequent section notes how the isolated molecule partition functions should be used to obtain the chemical potentials at the required concentrations.

As suggested above, the fundamental issue is the use of the cluster calculation $\text{Fe}(\text{H}_2\text{O})_6^{3+}$ to obtain the chemical potential, $\mu_{\text{Fe}^{3+}}$, of the hydrated ferric ion, Fe^{3+} . It is clear on physical grounds that such an approach should be advantageous when the identification of a relevant cluster is physically obvious and when the inner shell of the cluster requires a specialized treatment. What happens when the relevant cluster is not so obvious? What about cases when more than one cluster should be considered? How might this approach be justified more fully and how might the calculations be improved?

The statistical mechanical topic underlying the considerations here is that of association equilibrium [45,46,47] and is often associated with considerations [48] of ‘physical clusters.’ A suitable clustering definition [45,49] is required for these discussions to be explicit and heavier statistical mechanical formalisms can be deployed [45,46,47]. However, the treatment here aims for maximal simplicity. This argument is an adaptation of the potential distribution theorem [50].

In order to involve information on clusters, we express the density of interest in terms of cluster concentrations. Thus, if the Fe^{3+} ion appears only once in each cluster, *i.e.* if *mononuclear* clusters need be considered, then we would write

$$\rho_{\text{Fe}^{3+}} = \sum_M \rho_M \tag{8}$$

where M identifies a molecular cluster considered and the sum is over all molecular clusters that can form. A satisfactory clustering definition [45,49] insures that each ferric ion can be assigned to only one molecular cluster, *e.g.* that a molecular cluster with one ferric ion and six water molecules is not counted as six clusters of a ferric ion with five water molecules. The calculations above assumed $M = \text{Fe}(\text{H}_2\text{O})_6^{3+}$, and that was it. In the more general case that not all clusters are mononuclear, Eq. 8 would involve the obvious stoichiometric

coefficients. The concentrations ρ_M are obtained from

$$\rho_M = z_{Fe^{3+}} z_W^{n_M} (q_M/V) \left\langle \left\langle e^{-\Delta U/RT} \right\rangle \right\rangle_{0,M}. \quad (9)$$

n_M is the number of water molecules in the cluster of type M , (six in the example carried long here); $z_{Fe^{3+}}$ and z_W are the activity of the ferric ion and the water, respectively; *i.e.* $z_\gamma = e^{\mu_\gamma/RT}$; $q_M = q_M(T)$ is a conventionally defined canonical partition function for the cluster of type M [45,46,47,49]. The indicated average utilizes the thermal distribution of cluster and solvent under the conditions that there is no interaction between them. ΔU is the potential energy of interaction between the cluster and the solvent. In the example carried along here we do not pay attention to any counter-ions since those issues are tangential to the current considerations.

Eq. 9 is most conveniently derived by considering a grand ensemble. Suppose we have a definite clustering criterion: a cluster of a ferric ion and n_M water molecules is formed when exactly n_M water molecules are within a specified distance d of a ferric ion. In the example we have been carrying along, water molecules with oxygens within about 2.2 Å of a ferric ion are in chemical interaction with the ferric ion. It would be natural to specify $d \leq 2.2$ Å for clustered ferric-water(oxygen) distances. The average number $\langle N_M \rangle$ of such clusters is composed as

$$\begin{aligned} \Xi(z_{Fe^{3+}}, z_W, T, V) \langle N_M \rangle &= z_{Fe^{3+}} z_W^{n_M} \\ &\times \sum_{N_{Fe^{3+}} \geq 1, N_W \geq n_M} N_{Fe^{3+}} z_{Fe^{3+}}^{N_{Fe^{3+}}-1} \binom{N_W}{n_M} z_W^{N_W-n_M} Q(\mathbf{N}, V, T | n_M + 1) \end{aligned} \quad (10)$$

Here $\Xi(z_{Fe^{3+}}, z_W, T, V)$ is the grand canonical partition function; $N_{Fe^{3+}}$ is the number of ferric ions in the systems and N_W is the number of water molecules; $Q(\mathbf{N}, V, T | n_M + 1)$ is the canonical ensemble partition function with one specific ferric ion and n_M specific water molecules constrained to be clustered. The binomial coefficient $\binom{N_W}{n_M}$ provides the number of n_M -tuples of water molecules that can be selected from N_W water molecules. Because of the particle number factors in the summand the partition function there can also be considered to be the partition function for $N - 1$ ferric ions and $N_W - n_M$ water molecules but with

an extra $n_M + 1$ objects that constitute the cluster of interest. A reasonable distribution of those $n_M + 1$ extraneous objects is the distribution they would have in an ideal gas phase; the Boltzmann factor for that distribution appears already in the integrand of the $Q(\mathbf{N}, V, T | n_M + 1)$ and the normalizing denominator for that distribution is $n_M! q_M(T)$. The acquired factor $n_M!$ cancels the remaining part of the combinatorial $\binom{N_W}{n_M}$. Adjusting the dummy summation variables then leads to Eq. 9.

If we were to identify an activity for an M-cluster as $z_M = z_{Fe^{3+}} z_W^{n_M}$ we would obtain from Eq. 9 the general statistical thermodynamic formulae of Reference [44].

A virtue of the derivation of Eq. 9 sketched here is that the primordial activities $z_{Fe^{3+}}$ and z_W are clear from the beginning. This helps in the present circumstance where concentrations and chemical potentials of many other species and combinations will be of interest also.

Combining our preceding results, we obtain

$$\frac{\rho_{Fe^{3+}}}{z_{Fe^{3+}}} = \sum_M z_W^{n_M} (q_M/V) \langle\langle e^{-\Delta U/RT} \rangle\rangle_{0,M}. \quad (11)$$

This is a reexpression according to clusters of a basic result known both within the context of the potential distribution theorem [50] and diagrammatic (mathematical) cluster expansions. For the latter context see Eq. 2.7 of Reference [47]. Rearranging, we obtain the desired chemical potential

$$\mu_{Fe^{3+}} = -RT \ln \left[\sum_M \left(\frac{z_W^{n_M} q_M}{\rho_{Fe^{3+}} V} \right) \langle\langle e^{-\Delta U/RT} \rangle\rangle_{0,M} \right]. \quad (12)$$

This is the result that was sought. If higher-order clusters had been considered with a suitable clustering definition, the final result would have involved a more general polynomial of $z_{Fe^{3+}}$; higher powers of $z_{Fe^{3+}}$ would appear in the sums that would replace Eq. 8 because of the presence of higher powers of $z_{Fe^{3+}}$ in some instances of Eq. 9. A virtue of Eq. 12 result is that the thermodynamic activity of the water appears explicitly and that contribution may be included in a variety of convenient ways, perhaps utilizing experimental results. Furthermore, we see that there is no question whether a particular standard state for the water is relevant or, for example, whether only the excess part of the chemical potential of the water is required.

Notice that if the cluster definition had been restrictive enough that only the atomic $M=\text{Fe}^{3+}$ were present in appreciable concentration, *i.e.* $n_M=0$ for all clusters that need be considered, then Eq. 12 produces the previously known general answer for the chemical potential of a ferric ion in solution [44,50]:

$$\mu_{\text{Fe}^{3+}}/RT = \ln[\rho_{\text{Fe}^{3+}}V/q_{\text{Fe}^{3+}}] - \ln \langle e^{-\Delta U/RT} \rangle_0 \quad (13)$$

It would be natural to choose the electronic energy of the atomic ferric ion as the zero of energy and to anticipate that the degeneracy of the electronic degrees of freedom will be physically irrelevant. Then it would be sufficient to put $V/q_{\text{Fe}^{3+}} = \Lambda_{\text{Fe}^{3+}}^3 = (h^2/2\pi m_{\text{Fe}^{3+}} RT)^{3/2}$, the cube of the deBroglie wavelength of the ferric ion. $m_{\text{Fe}^{3+}}$ is the mass of the ion, and h is the Planck constant. In any case, we define the absolute free energy of the hydrated ferric ion as the second term on the right $\Delta\mu_{\text{Fe}^{3+}} = -RT \ln \langle e^{-\Delta U/RT} \rangle_0$. In view of Eq. 7 we then have

$$\Delta\mu_{\text{Fe}^{3+}} = RT \ln \left[\frac{q_{\text{Fe}^{3+}}}{q_M} \right] - RT \ln \langle \langle e^{-\Delta U/RT} \rangle \rangle_{0,M} - 6\mu_W, \quad (14)$$

where $M=\text{Fe}(\text{H}_2\text{O})_6^{3+}$. This Eq. 14 is the formula that was used.

A generalization of interest is the case that the solvent contains more than one species that may complex with a specific metal ion. For example, suppose that ammonia may be present in addition to water, that mixed complexes may form with ferric ion, and that these complexes have been studied as clusters in the same way that the hexaquo ferric ion complex was studied above. Then the result Eq. 12 is straightforwardly generalized by including the proper combinations of activities of the additional ligands possible.

Standard State Modifications

Many *ab initio* electronic structure packages, such as the Gaussian94 package used here, can produce molecular (or cluster) partition functions $q_M = q_M(T)$ and on this basis free energies for the species and reactions considered. It should be emphasized that these are typically applicable to a hypothetical ideal gas at concentrations corresponding to pressure

p=1 atm, see Table III. Thus, for example, these results determine the ideal chemical potential $\mu_W = RT \ln[\rho_W V/q_W(T)]$. However, because of the choice of hypothetical p=1 atm ideal gas standard state, those results use $\rho_W = p/RT$ with p=1 atm. In Gaussian94, for example, this logarithmic concentration dependence is considered a translational entropy contribution and, therefore, the entropic contribution to the reaction free energy of the first reaction in Table III is substantial and unfavorable. Because of the dilute reaction medium associated with p=1 atm, the water molecules written as reactants in this reaction have more freedom before complexation than they do after. This is an entirely expected physical effect but inappropriate in solution. To obtain results applicable at the concentration of liquid water we determine that pressure parameter $p = \rho_W RT$ from the experimental density of liquid water $\rho_W = 997.02 \text{ kg/m}^3$. The required value is p=1354 atm as indicated in Table IV. When this value is utilized in the expression for the translational entropy contributions, the translational entropy penalty of Table III for the first reaction is about half recovered. Because the second through fifth reactions of Table III were written to have the same molecule numbers for reactions and products this translational entropy contribution is very minor in those cases.

We note also that the experimental tabulation of Reference [10] suggested as an experimental result for the absolute free energy of the hydrated ferric ion (-1037 kcal/mol) of Table IV requires an adjustment of about 1.9 kcal/mol [24,42] for similar reasons. This adjustment is insignificant for that property with the methods used here.

References and Notes

- [1] J. R. Rustad, B. P. Hay, and J. W. Halley. *J. Chem. Phys.*, 102:427, 1995.
- [2] J. R. Rustad, A. R. Felmy, and B. P. Hay. *Geochemica et Cosmochemica Acta*, 60:1553, 1996.
- [3] J. R. Rustad, A. R. Felmy, and B. P. Hay. *Geochemica et Cosmochemica Acta*, 60:563, 1996.

- [4] R. A. Marcus. *Faraday Discuss. Chem. Soc.*, 74:7, 1982.
- [5] H. L. Friedman and M. D. Newton. *Faraday Discuss. Chem. Soc.*, 74:73, 1982.
- [6] J. A. Jafri, J. Logan, and M. D. Newton. *Isr. J. Chem. Symp.*, 19:340, 1980.
- [7] M. D. Newton. *Int. J. Quant. Chem. Symp.*, 14:363, 1980.
- [8] J. Silverman and R. W. Dodson. *J. Phys. Chem.*, 56:846, 1952.
- [9] C. M. Flynn. *Chem. Rev.*, 84:31, 1984.
- [10] H. L. Friedman and V. V. Krishnan. *Water: A comprehensive treatise*. Plenum, NY, 1973.
- [11] E. S. Marcos, J. M. Martinez, and R. R. Papalardo. *J. Phys. Chem.*, 105:5968, 1996.
- [12] A. D. Becke. *J. Chem. Phys.*, 98:5648, 1993.
- [13] M. J. Frisch, G. W. Trucks, H. B. Schlegel, P. M. W. Gill, B. G. Johnson, M. A. Robb, J. R. Cheeseman, T. A. Keith, G. A. Petersson, J. A. Montgomery, K. Raghavachari, M. A. Al-Laham, V. G. Zakrzewski, J. V. Ortiz, J. B. Foresman, J. Cioslowski, B. B. Stefanov, A. Nanayakkara, M. Challacombe, C. Y. Peng, P. Y. Ayala, W. Chen, M. W. Wong, J. L. Andres, E. S. Replogle, R. Gomperts, R. L. Martin, D. J. Fox, J. S. Binkley, D. J. Defrees, J. Baker, J. J. P. Stewart, M. Head-Gordon, C. Gonzalez, and J. A. Pople. *Gaussian 94 (Revision D.1)*. Gaussian, Inc., Pittsburgh, PA, 1995.
- [14] A. Ricca and C. W. Bauschlicher. *J. Phys. Chem.*, 98:12899, 1994.
- [15] T. V. Russo, R. L. Martin, and P. J. Hay. *J. Chem. Phys.*, 102:8023, 1995.
- [16] A. J. H. Wachters. *J. Chem. Phys.*, 52:1033, 1970.
- [17] P. J. Hay. *J. Chem. Phys.*, 66:4377, 1977.
- [18] C. M. Brenneman and K. B. Wiberg. *J. Comp. Chem.*, 8:894, 1987.

- [19] G. Hummer L. R. Pratt and A. E. García. *Biophys. Chem.*, 51:147, 1994.
- [20] G. J. Tawa and L. R. Pratt. Structure and reactivity in aqueous solution: Characterization of chemical and biological systems. volume 568 of *ACS Symposium Series*, page 60, Washington, DC, 1994. American Chemical Society.
- [21] G. J. Tawa and L. R. Pratt. *J. Am. Chem. Soc.*, 117:1625, 1995.
- [22] G. Hummer, L. R. Pratt, and A. E. García. *J. Phys. Chem.*, 99:14188, 1995.
- [23] S. A. Corcelli, J. D. Kress, L. R. Pratt, and G. J. Tawa. Pacific symposium on bio-computing '96. pages 142–159, River Edge, NJ, 1995. World Scientific.
- [24] G. Hummer, L. R. Pratt, and A. E. García. *J. Phys. Chem.*, 100:1206, 1996.
- [25] G. J. Tawa, R. L. Martin, L. R. Pratt, and T. V. Russo. *J. Phys. Chem.*, 100:1515, 1996.
- [26] G. Hummer, L. R. Pratt, A. E. García, B. J. Berne, and S. W. Rick. *J. Phys. Chem. B*, 101:3017, 1997.
- [27] L. R. Pratt, G. J. Tawa, G. Hummer, A. E. García, and S. A. Corcelli. *Int. J. Quant. Chem.*, 64:121, 1997.
- [28] G. Hummer, L. R. Pratt, and A. E. García. *J. Chem. Phys.*, LA-UR-96-1591:(in press), 1997.
- [29] G. Hummer, L. R. Pratt, and A. E. García. *J. Am. Chem. Soc.*, 119:8523, 1997.
- [30] E. V. Stefanovich and T. N. Truong. *Chem. Phys. Letts.*, 244:65, 1995.
- [31] R. Åkesson, L. G. M. Pettersson, M. Sandström, and U. Wahlgren. *J. Am. Chem. Soc.*, 116:8691, 1994.
- [32] J. Li, C. L. Fisher, J. L. Chen, D. Bashford, and L. Noodleman. *Inorg. Chem.*, 35:4694, 1996.

- [33] G. J. Herdman and G. W. Neilson. *J. Phys.: Condens. Matter*, 4:627, 1992.
- [34] B. S. Brunschwig, C. Creutz, D. H. Macartney, T.-K. Sham, and N. Sutin. *Faraday Discuss. Chem. Soc.*, 74:113, 1982.
- [35] H. Ohtaki and T. Radnai. *Chem. Rev.*, 93:1157, 1993.
- [36] R. Åkesson, L. G. M. Pettersson, M. Sandström, and U. Wahlgren. *J. Phys. Chem.*, 96:150, 1992.
- [37] R. Åkesson, L. G. M. Pettersson, M. Sandström, P. Siegbahn, and U. Wahlgren. *J. Phys. Chem.*, 96:10773, 1992.
- [38] T. Ziegler. *Chem. Rev.*, 91:651, 1991.
- [39] C. Sosa, J. Andzelm, B. C. Elkin, E. Wimmer, K. D. Dobbs, and D. A. Dixon. *J. Phys. Chem.*, 96:6630, 1992.
- [40] D. R. Rosseinsky. *Chem. Rev.*, 65:467, 1965.
- [41] J. J. Urban and J. R. Damewood, Jr. *J. Chem. Soc. Chem. Comm.*, page 1636, 1990.
- [42] Y. Marcus. *Biophys. Chem.*, 51:111, 1994.
- [43] A. Meagher. *Inorg. Chim. Acta*, 146:19, 1988.
- [44] L. R. Pratt. *Encyclopedia of computational chemistry*. Wiley, NY, 1997.
- [45] F. H. Stillinger Jr. *J. Chem. Phys.*, 38:1486, 1963.
- [46] D. Chandler and L. R. Pratt. *J. Chem. Phys.*, 65:2925, 1976.
- [47] L. R. Pratt and D. Chandler. *J. Chem. Phys.*, 66:148, 1977.
- [48] T. L. Hill. *Statistical Mechanics*. Dover, 1956. See section 27.
- [49] R. A. LaViolette and L. R. Pratt. *Phys. Rev. A*, 28:2482, 1983.

- [50] B. Widom. *J. Phys. Chem.*, 86:869–872, 1982.
- [51] S. Liu Y. Bu and X. Song. *Chem. Phys. Letts.*, 227:121, 1994.
- [52] K. Mandix and H. Johansen. *J. Phys. Chem.*, 96:7261, 1992.
- [53] W. M. Latimer, K. S. Pitzer, and C. M. Slansky. *J. Chem. Phys.*, 7:108, 1939.
- [54] P.M.W. Gill, B.G. Johnson, J.A. Pople, and M.J. Frisch. *Int. J. Quantum Chem. Symp.*, 26:319, 1992.
- [55] L.A. Curtiss, K. Raghavachari, G.W. Trucks, and J.A. Pople. *J. Chem. Phys.*, 94:7221, 1991.

FIGURES

Figure 1. Computed structure of the $\text{Fe}(\text{H}_2\text{O})_6$ complex.

Figure 2. Computed structure of the $\text{Fe}(\text{H}_2\text{O})_5\text{OH}^{2+}$ complex.

Figure 3. Computed structures of the $\text{Fe}(\text{H}_2\text{O})_4\text{OH}^{2+}$ complexes; *cis* (upper), *outer* sphere (middle), *trans* (lower), in order from lowest to highest energy.

Figure 4. Computed structure of the penta-coordinate $\text{Fe}(\text{H}_2\text{O})_3(\text{OH})_2^+$ complex. This should be compared to the middle structure of Figure 3.

TABLES

TABLE I: Electronic energy (E /[au]), Zero-point energy (ZPE/[kcal/mole]), and excess chemical potential (μ^* /[kcal/mol]) with the B3LYP and dielectric continuum solvation approximations. Dielectric radii for all atoms were taken from Ref. [30] except $R_{Fe}=2.08\text{\AA}$.

	E	ZPE	μ^*
H	-0.497885	–	–
Fe ³⁺	-1261.590210	–	–
H ₂ O	-76.434010	13.3	-8.3
H ₃ O ⁺	-76.707704	21.5	-96
OH	-75.739116	5.2	–
OH [–]	-75.802535	4.5	-108
Fe(H ₂ O) ₆ ³⁺	-1721.261664	94.3	-441
Fe(H ₂ O) ₅ OH ²⁺	-1721.216989	85.6	-203
<i>cis</i> Fe(H ₂ O) ₄ (OH) ₂ ⁺	-1720.987174	79.1	-71
<i>trans</i> Fe(H ₂ O) ₄ (OH) ₂ ⁺	-1720.983894	78.3	-74
<i>outer</i> Fe(H ₂ O) ₄ (OH) ₂ ⁺	-1720.985680	79.0	-73
Fe(H ₂ O) ₃ (OH) ₂ ⁺	-1644.536430	62.8	-69

TABLE II: Gas-phase thermochemistries (ΔE_0 , kcal/mole) in the B3LYP approximation. Note that these include zero-point energy. The ionization potential (IP) of hydrogen and electron affinity (EA) of the hydroxyl radical are in eV.

	ΔE_0	Expt. [54,55]
$\text{H}_2\text{O} \rightarrow \text{H} + \text{OH}$	115.5	118.0
$\text{H}_2\text{O} \rightarrow \text{H}^+ + \text{OH}^-$	387.5	389.3
$\text{H}_2\text{O} + \text{H}^+ \rightarrow \text{H}_3\text{O}^+$	-163.5	-165.1
$2\text{H}_2\text{O} \rightarrow \text{H}_3\text{O}^+ + \text{OH}^-$	223.9	224.0
IP(H)	13.55	13.6
EA(OH)	1.76	1.83

TABLE III: Ideal gas thermochemistries (kcal/mole) at T=298.15 K and p=1 atm, utilizing the B3LYP approximation. The first column gives the electronic energy contribution, the second includes the zero-point energy, the third evaluates the energy at 298.15K, the fourth gives the enthalpy at 298.15K, and the fifth column is the Gibbs free energy.

	ΔE_e	ΔE_0	ΔE_{298}	$\Delta H_{298}^{(0)}$	$\Delta G_{298}^{(0)}$
$\text{Fe}^{3+} + 6\text{H}_2\text{O} \rightarrow \text{Fe}(\text{H}_2\text{O})_6^{3+}$	-669.8	-655.2	-657.2	-660.8	-601.6
$\text{Fe}(\text{H}_2\text{O})_6^{3+} + \text{H}_2\text{O} \rightarrow \text{Fe}(\text{H}_2\text{O})_5\text{OH}^{2+} + \text{H}_3\text{O}^+$	-143.7	-144.2	-143.2	-143.2	-148.4
$\text{Fe}(\text{H}_2\text{O})_5\text{OH}^{2+} + \text{H}_2\text{O} \rightarrow \textit{cis} \text{Fe}(\text{H}_2\text{O})_4(\text{OH})_2^+ + \text{H}_3\text{O}^+$	-27.5	-25.8	-26.6	-26.6	-25.7
$\text{Fe}(\text{H}_2\text{O})_5\text{OH}^{2+} + \text{H}_2\text{O} \rightarrow \textit{trans} \text{Fe}(\text{H}_2\text{O})_4(\text{OH})_2^+ + \text{H}_3\text{O}^+$	-25.5	-24.5	-25.0	-25.0	-24.9
$\text{Fe}(\text{H}_2\text{O})_5\text{OH}^{2+} + \text{H}_2\text{O} \rightarrow \textit{outer} \text{Fe}(\text{H}_2\text{O})_4(\text{OH})_2^+ + \text{H}_3\text{O}^+$	-26.6	-25.0	-25.5	-25.5	-25.9
$\textit{outer} \text{Fe}(\text{H}_2\text{O})_5\text{OH}^{2+} \rightarrow \text{Fe}(\text{H}_2\text{O})_3(\text{OH})_2^+ + \text{H}_2\text{O}$	9.6	6.7	6.7	7.3	-1.8

TABLE IV: Aqueous reaction thermochemistries (kcal/mole) at T=298.15 K utilizing the B3LYP approximation. The first column gives the gas-phase free energy from Table III, the second reports the net free energy after adjustment for the alternative concentration in the liquid (“p=1354 atm” for the water species), and the third column gives the solvation increment to the free energy, *i.e.* that contribution due to solute-solvent interactions. Experimental results are given in the final column. The solution phase results of the first row are the “absolute free energies of the hydrated ferric ion.” See the appendix, Eq. (7) for interpretation.

	$\Delta G_{298}^{(0)}$	ΔG_{298}	μ^*	$\Delta G_{298} + \mu^*$	Expt. [54,55]
$\text{Fe}^{3+} + 6\text{H}_2\text{O} \rightarrow \text{Fe}(\text{H}_2\text{O})_6^{3+}$	-601.6	-628.9	-391.2	-1020.1	-1019,-1037
$\text{Fe}(\text{H}_2\text{O})_6^{3+} + \text{H}_2\text{O} \rightarrow \text{Fe}(\text{H}_2\text{O})_5\text{OH}^{2+} + \text{H}_3\text{O}^+$	-148.4	-148.7	150.3	1.6	3
$\text{Fe}(\text{H}_2\text{O})_5\text{OH}^{2+} + \text{H}_2\text{O} \rightarrow \textit{cis} \text{Fe}(\text{H}_2\text{O})_4(\text{OH})_2^{1+} + \text{H}_3\text{O}^+$	-25.7	-26.0	44.3	18.3	5
$\text{Fe}(\text{H}_2\text{O})_5\text{OH}^{2+} + \text{H}_2\text{O} \rightarrow \textit{trans} \text{Fe}(\text{H}_2\text{O})_4(\text{OH})_2^{1+} + \text{H}_3\text{O}^+$	-24.9	-25.2	41.3	16.1	
$\text{Fe}(\text{H}_2\text{O})_5\text{OH}^{2+} + \text{H}_2\text{O} \rightarrow \textit{outer} \text{Fe}(\text{H}_2\text{O})_4(\text{OH})_2^{1+} + \text{H}_3\text{O}^+$	-25.9	-26.1	42.3	16.3	
$\textit{outer} \text{Fe}(\text{H}_2\text{O})_5\text{OH}^{2+} \rightarrow \text{Fe}(\text{H}_2\text{O})_3(\text{OH})_2^{1+} + \text{H}_2\text{O}$	-1.8	+2.7	-4.3	-1.6	

TABLE V: Selected geometrical parameters for species in $\text{Fe}(\text{H}_2\text{O})_6$ hydrolysis reactions from B3LYP calculations.

	R(Fe-OH ₂)Å	R(Fe-OH)Å	$\theta(\text{OH-Fe-OH})$	$\theta_{\textit{tilt}}(\text{H}_2\text{O})^1$
$\text{Fe}(\text{H}_2\text{O})_6^{3+}$	2.060	–	–	0(6)
$\text{Fe}(\text{H}_2\text{O})_5\text{OH}^{2+}$	2.103 – 2.150	1.760	–	0(3),30(2)
$\textit{cis} \text{Fe}(\text{H}_2\text{O})_4(\text{OH})_2^{1+}$	2.172 – 2.296	1.820 – 1.847	108	36,40,44,51
$\textit{trans} \text{Fe}(\text{H}_2\text{O})_4(\text{OH})_2^{1+}$	2.168 – 2.194	1.851	180	38(2),44(2)
$\textit{outer} \text{Fe}(\text{H}_2\text{O})_4(\text{OH})_2^{1+}$	2.108 – 2.196	1.811	114	18,44,44
$\text{Fe}(\text{H}_2\text{O})_3(\text{OH})_2$	2.102 – 2.185	1.803 – 1.807	128	22,40,40

¹Defined as O-H₁-H₂-Fe dihedral angle.

TABLE VI: Atomic charges from ChelpG analysis of the electrostatic potential.

	Fe(H ₂ O) ₆	Fe(H ₂ O) ₅ OH	Fe(H ₂ O) ₄ (OH) ₂	Fe(H ₂ O) ₄ (OH) ₂	Fe(H ₂ O) ₄ (OH) ₂	Fe(H ₂ O) ₃ (OH) ₂
			<i>cis</i>	<i>trans</i>	<i>outer</i>	
Fe	+2.15	+1.62	+1.14	+1.54	+1.24	+0.92
O2	-1.02	-0.88	-0.69	-0.85	-0.69	-0.63
H8	+0.58	+0.50	+0.43	+0.47	+0.41	+0.41
H9	+0.58	+0.52	+0.42	+0.48	+0.42	+0.42
O3	-1.02	-0.88	-0.68	-0.89	-0.69	-0.62
H10	+0.58	+0.50	+0.43	+0.49	+0.41	+0.41
H11	+0.58	+0.52	+0.42	+0.48	+0.42	+0.41
O4	-1.02	-0.78	-0.62	-0.86	-0.66	-0.48
H12	+0.58	+0.47	+0.40	+0.45	+0.42	+0.37
H13	+0.58	+0.47	+0.39	+0.48	+0.42	+0.37
O5	-1.02	-0.77	-0.71	-0.83	-0.88	–
H14	+0.58	+0.47	+0.43	+0.45	+0.45	–
H15	+0.58	+0.47	+0.42	+0.48	+0.45	–
O6	-1.02	-0.80	-0.82	-0.90	-0.77	-0.67
H16	+0.58	+0.47	+0.44	+0.45	+0.40	+0.39
H17	+0.58	+0.41	–	–	–	–
O7	-1.02	-0.97	-0.82	-0.89	-0.75	-0.68
H18	+0.58	+0.60	+0.44	+0.44	+0.38	+0.39
H19	+0.58	–	–	–	–	–

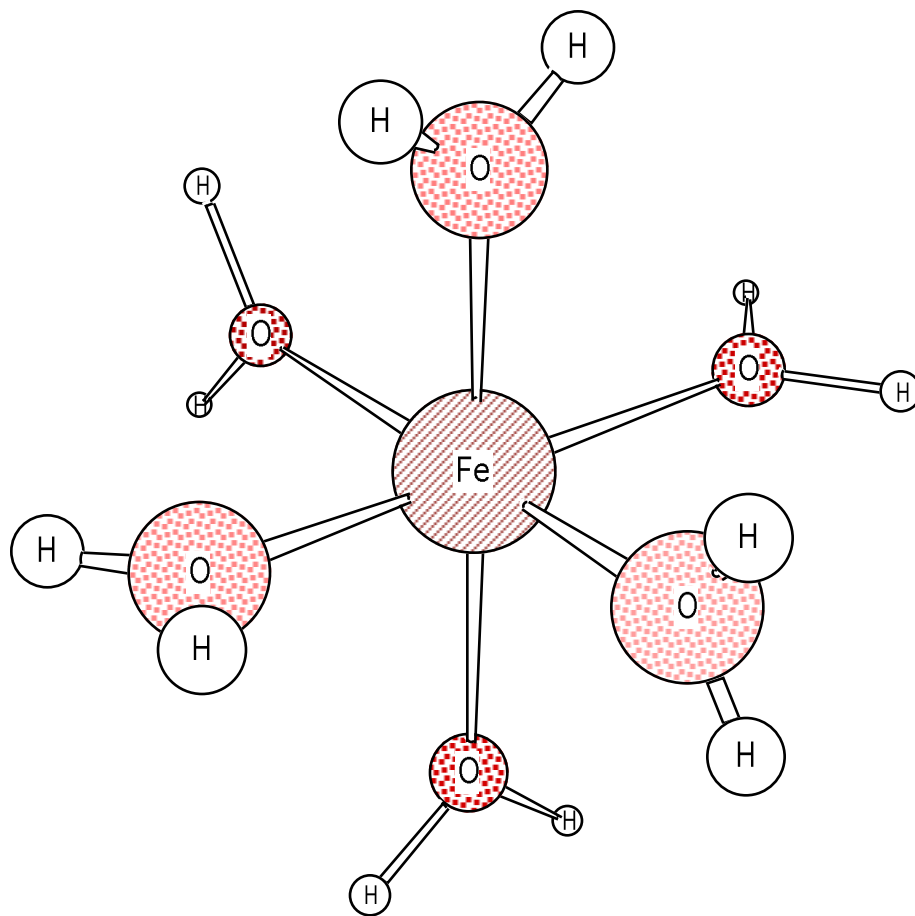


Figure 1

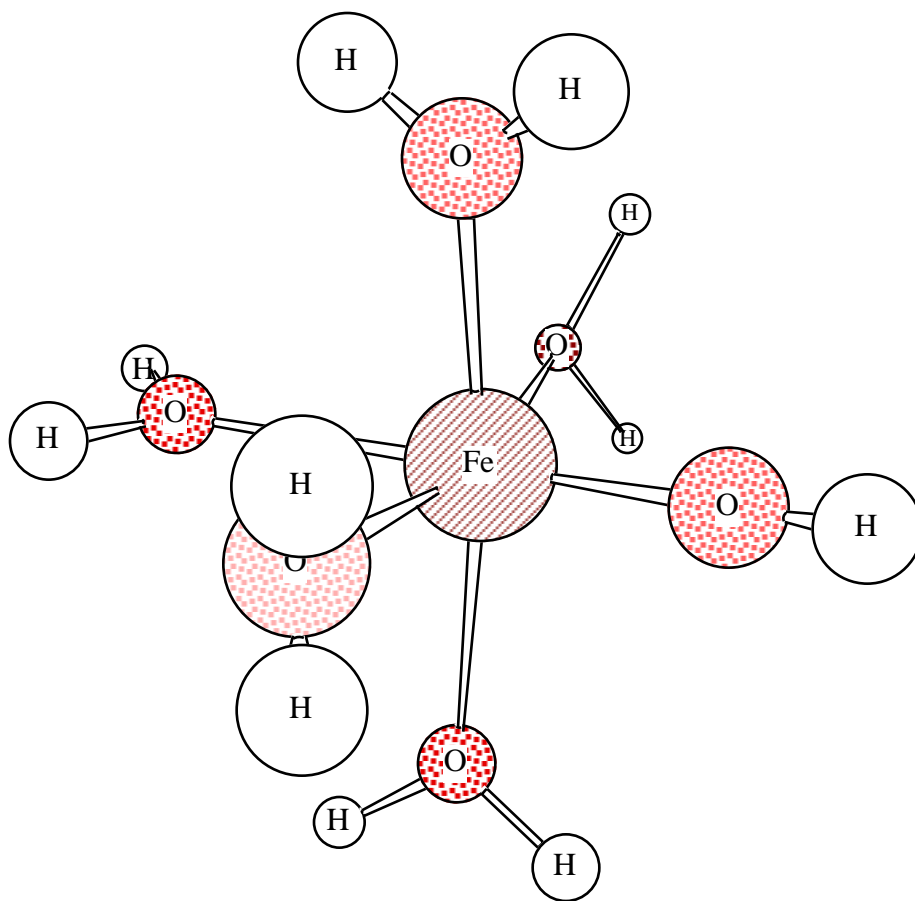


Figure 2

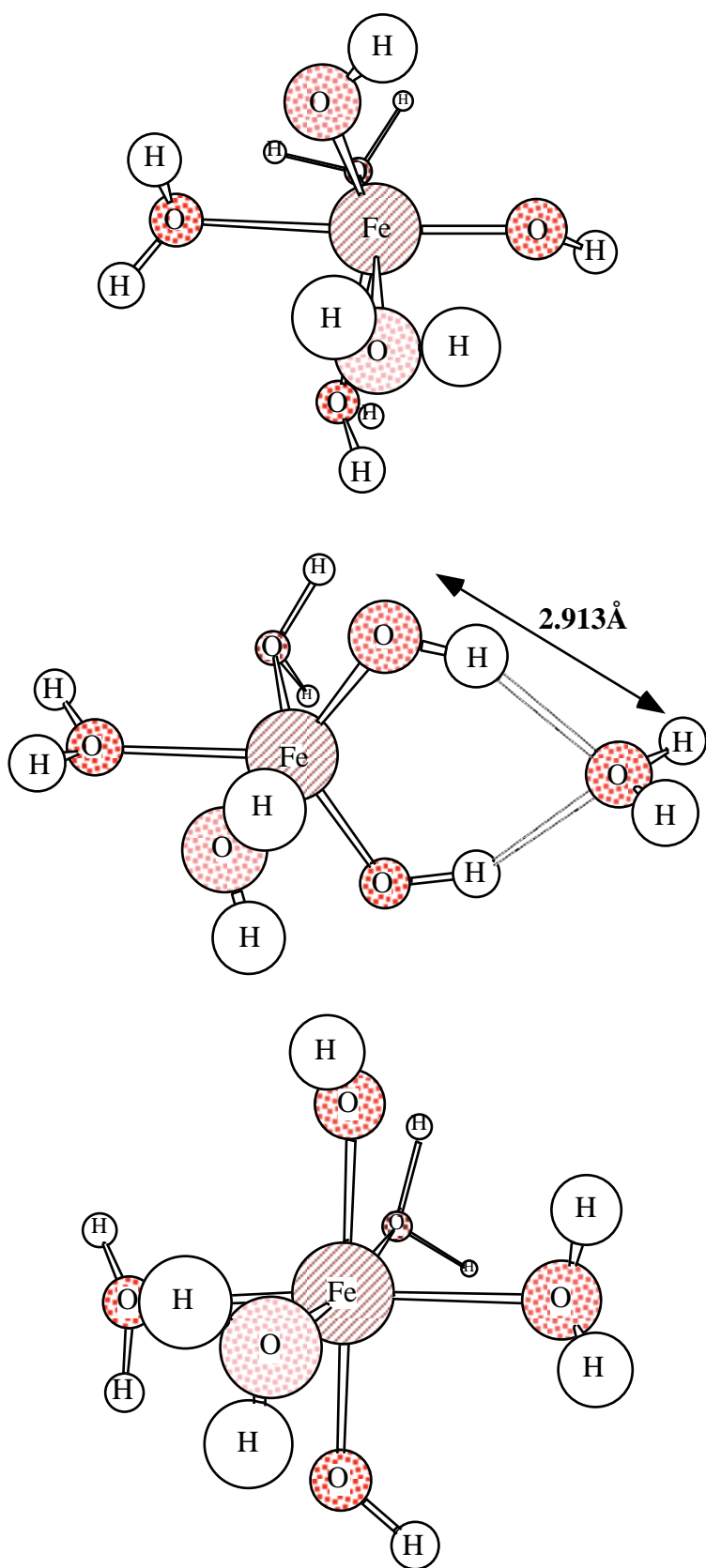


Figure 3

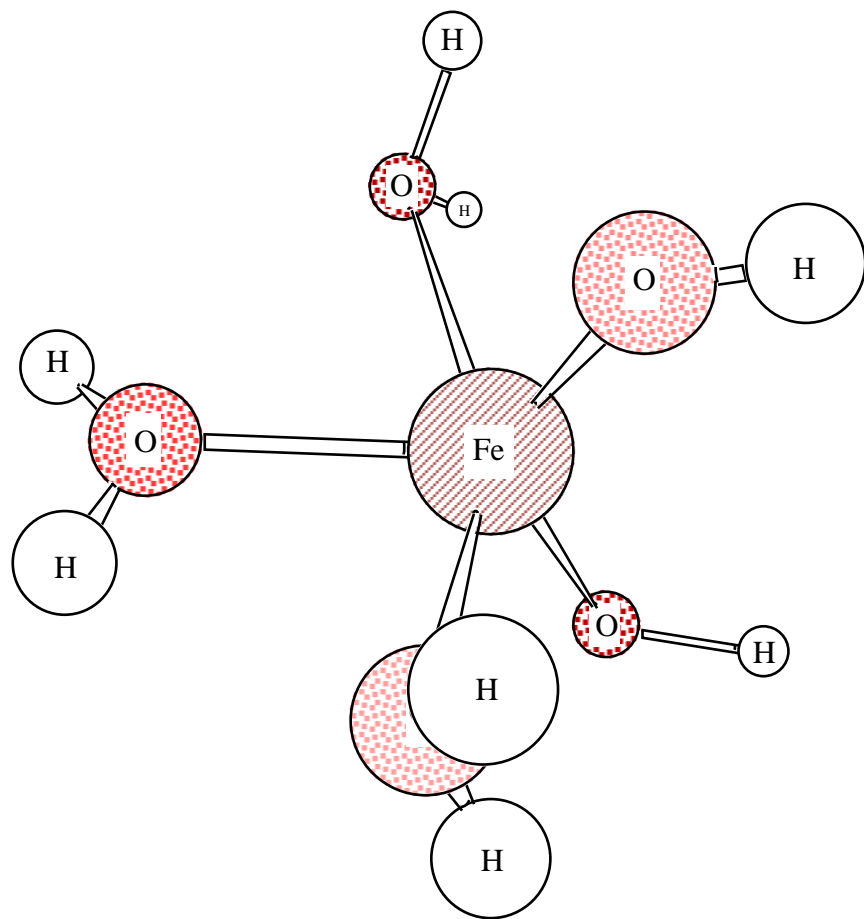


Figure 4